Portable EEG Correlates of Basketball Free-Throw Performance: Pilot Session Analysis Report

Lukas Laskowski Kyle E. Mathewson

February 20, 2026

Abstract

This report presents the analysis of a single pilot session recorded using the FreethrowEEG system. Continuous EEG band power (delta, theta, alpha, beta, gamma) was recorded from a Muse 2 headset while the participant performed 10 free throws (3 made, 7 missed; 30%). Shot-locked epochs were extracted and compared between successful and unsuccessful attempts. Concurrent video was analysed with MediaPipe pose estimation to extract biomechanical features aligned with neural dynamics. Descriptive statistics, time-series visualizations, pose kinematics, and exploratory inferential tests are reported.

1 Introduction

Electroencephalography (EEG) has been widely used to study neural correlates of motor performance, including precision sport tasks such as archery, shooting, and golf putting. A consistent finding in the literature is that successful performers exhibit distinct pre-performance EEG patterns, particularly reduced alpha desynchronization and modulated theta activity, compared to unsuccessful attempts. This pilot session tests whether such patterns are detectable using a portable, four-channel Muse 2 headset during basketball free-throw shooting.

The present analysis focuses on:

1. Visualizing continuous and shot-locked EEG band power;
2. Comparing pre-shot, execution, and post-shot neural signatures between made and missed free throws;
3. Evaluating the theta/alpha ratio as a candidate readiness marker;
4. Examining shot-by-shot band power progression across the session.

2 Methods

2.1 Participant and Task

The participant (lukas_test) performed 10 free throws during a single session lasting 5.8 minutes. Each trial followed a structured protocol: a preparation phase ($\sim$5 s), a pre-shot baseline ($\sim$5 s), shot execution ($\sim$2 s), post-shot recording ($\sim$3 s), and a review phase. Shot outcome (made/missed) was manually coded.

2.2 EEG Recording

EEG was recorded continuously using a Muse 2 headband (four channels: TP9, AF7, AF8, TP10; 256 Hz sampling rate). Band power was computed in real time using a 1-second sliding window with 25% overlap. A 4th-order Butterworth bandpass filter was applied to extract five standard frequency bands: delta (1–4 Hz), theta (4–8 Hz), alpha (8–13 Hz), beta (13–30 Hz), and gamma (30–50 Hz). Environmental line noise was removed via a Butterworth notch filter at 60 Hz. Power values were averaged across all four channels.

2.3 Video Recording and Pose Estimation

Video was recorded simultaneously at 30 fps (640×480, WebM/VP9 codec) using the device camera. The recording started with the session and timestamps in the EEG data file map directly to video time. Post-hoc pose estimation was performed using the MediaPipe Pose Landmarker (heavy model), extracting 33 body landmarks per frame. Biomechanical features—elbow angle (shoulder–elbow–wrist), wrist height, knee angle (hip–knee–ankle), and body lean angle (torso deviation from vertical)—were computed for each frame during the shot execution phase. Ball release was estimated as the frame where wrist velocity peaked while the wrist was near its highest position.

2.4 Analysis

Continuous EEG data were segmented into shot-locked epochs aligned to the onset of the execution phase. Epochs were interpolated onto a common time grid (-12 to $+8$ s relative to shot onset at 0.25 s resolution) and averaged separately for made and missed shots. Phase-wise mean power was compared using Welch's t-test (unequal variances) and the Mann–Whitney U test. Effect sizes are reported as Cohen's d. Given the pilot nature of this data set (10 shots), all inferential statistics should be interpreted with caution.

Individual shot clips were extracted from the video, and stop-motion frame sequences were generated for each trial. Average frame composites were created by pixel-averaging release-point frames within each outcome group. "Ghost" overlays show the variability in shooting form by superimposing skeleton renderings from all shots within a group.

3 Results

3.1 Session Overview

The participant completed 10 shots over 5.8 minutes (30% accuracy). Figure 1 shows the session timeline with shot phases and outcomes overlaid on the continuous alpha power trace.

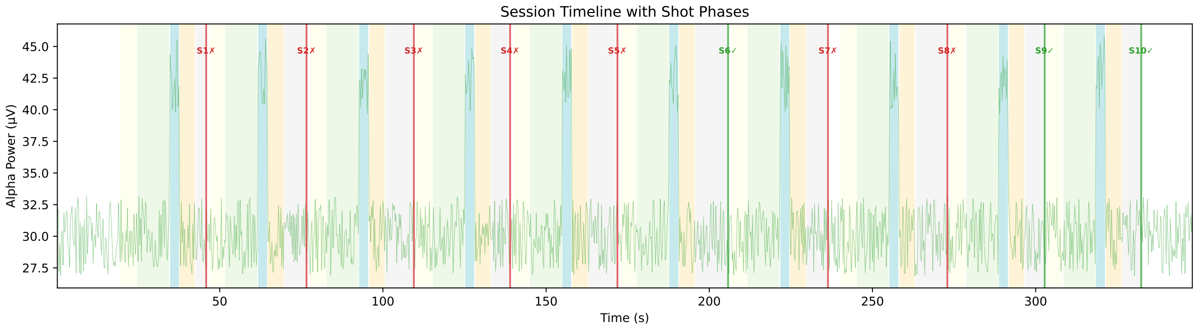

Figure 1: Session timeline. Each vertical line marks a shot (green = made, red = missed). Shaded regions indicate trial phases.

3.2 Continuous Band Power

Figure 2 shows the five frequency bands across the full session. Visual inspection of the continuous traces reveals characteristic fluctuations across all five bands over the 5.8-minute session.

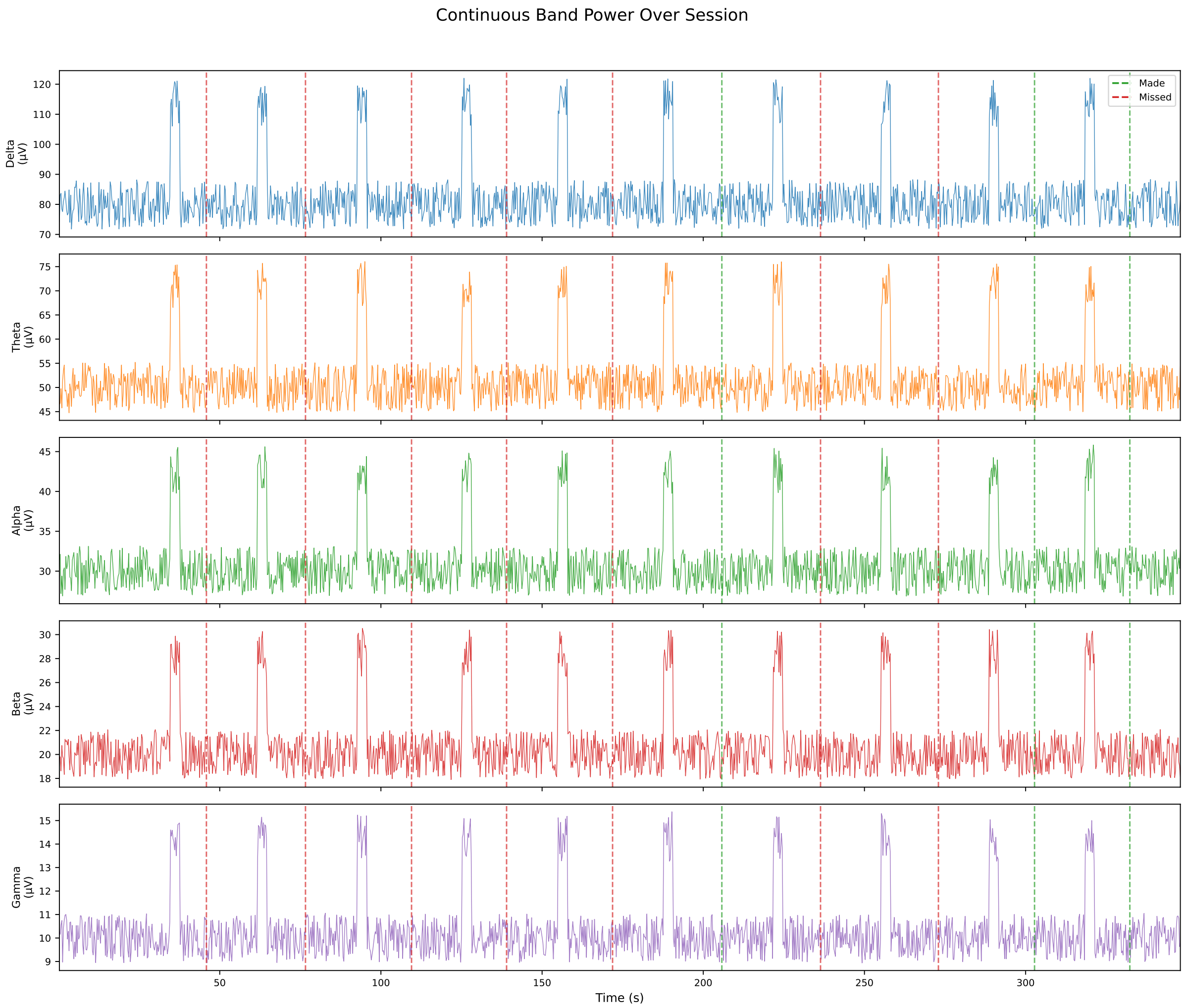

Figure 2: Continuous band power (delta through gamma) over the entire session. Dashed vertical lines indicate shot execution (green = made, red = missed).

3.3 Signal Filtering

Figure 3 demonstrates the effect of low-pass, high-pass, and bandpass Butterworth filtering applied to the raw delta-band signal from the first 60 seconds of the session.

Figure 3: Filtering demonstration on the raw delta signal: (a) unfiltered, (b) low-pass <1 Hz, (c) high-pass >0.5 Hz, (d) bandpass 0.5–1.5 Hz.

3.4 Shot-Locked Averages

Figure 4 shows mean band power (± SEM) locked to the onset of the execution phase, averaged across all 10 shots.

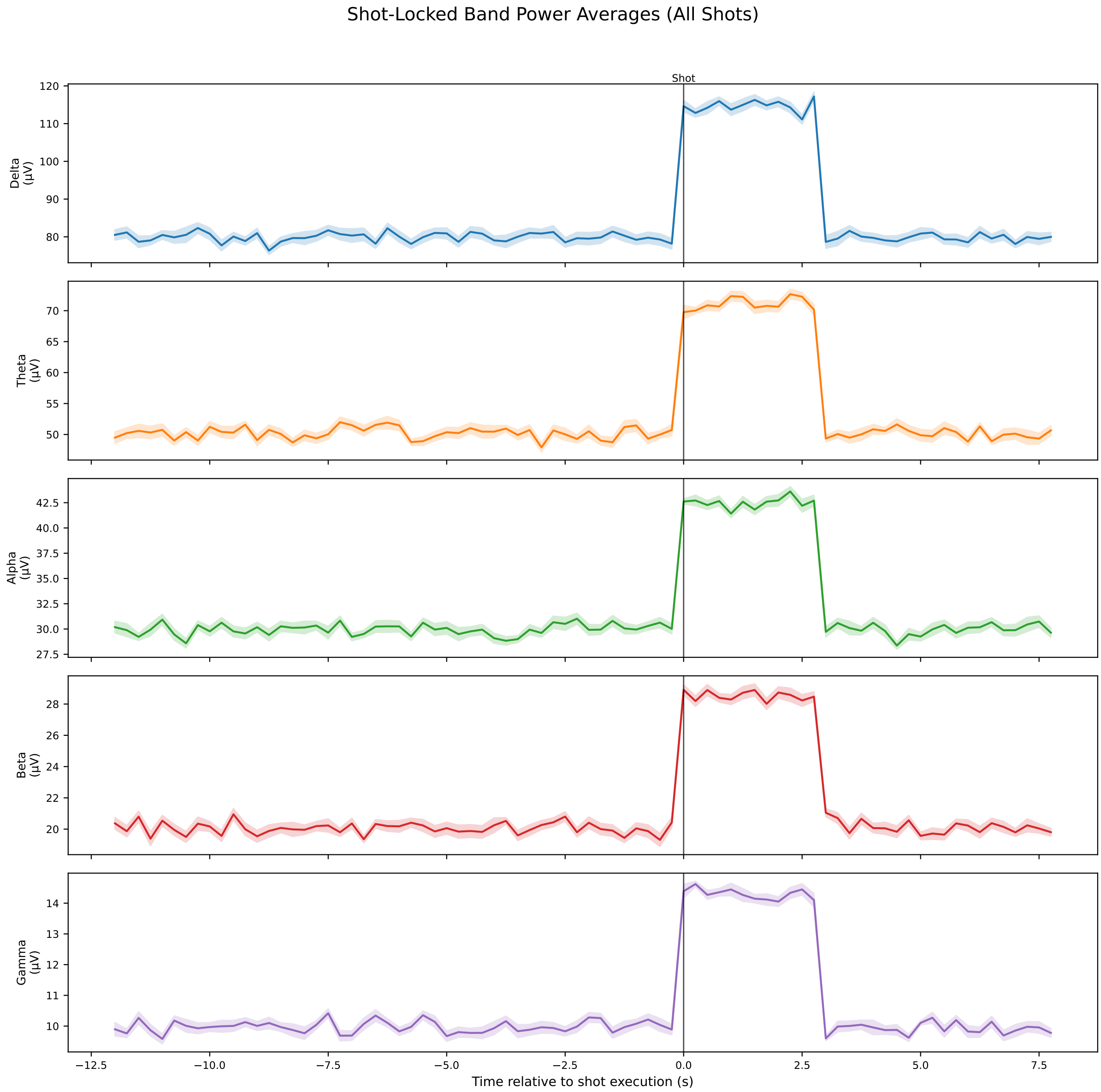

Figure 4: Shot-locked band power averages (all shots). Time 0 = execution onset. Shaded regions represent ±1 SEM.

3.5 Made vs. Missed Comparison

Figure 5 compares shot-locked averages for made and missed shots. delta power was 0.3% lower for made shots ($M = 79.7$) compared to missed ($M = 79.9$). theta power was 0.4% higher for made shots ($M = 50.4$) compared to missed ($M = 50.2$). alpha power was 0.2% lower for made shots ($M = 29.9$) compared to missed ($M = 30.0$). beta power was 0.4% lower for made shots ($M = 20.0$) compared to missed ($M = 20.1$). gamma power was 0.3% lower for made shots ($M = 10.0$) compared to missed ($M = 10.0$). No frequency band reached trend-level significance ($p < .10$) in the pre-shot comparison, consistent with the limited sample size.

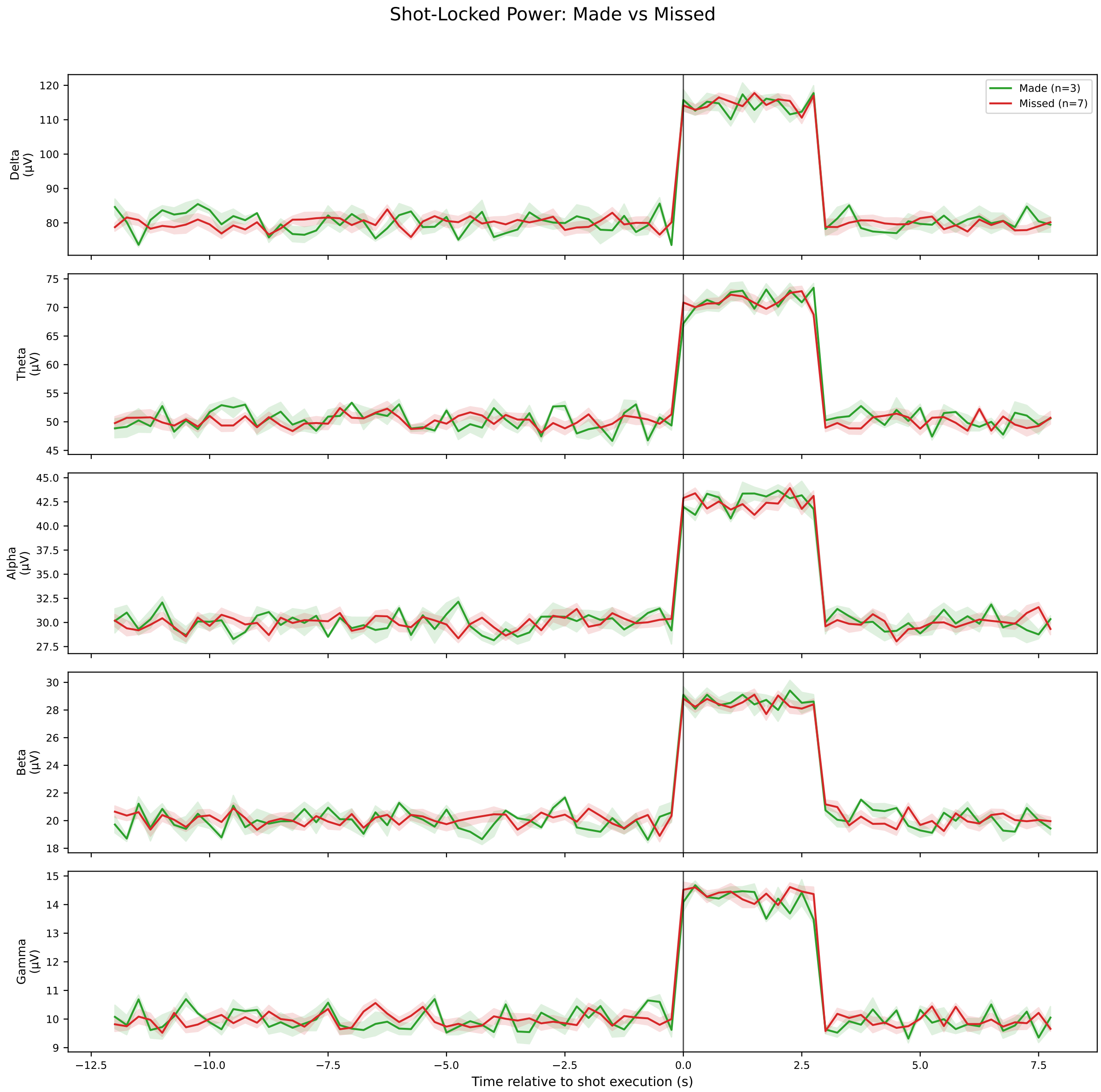

Figure 5: Shot-locked power comparison: made (green) vs. missed (red). Shaded regions are ±1 SEM.

3.6 Phase-Wise Analysis

Figure 6 displays mean power during the pre-shot, execution, and post-shot phases, broken down by outcome and frequency band. For made shots, delta power increased by 43.5% from pre-shot to execution. For made shots, theta power increased by 41.3% from pre-shot to execution. For made shots, alpha power increased by 42.4% from pre-shot to execution. For made shots, beta power increased by 43.4% from pre-shot to execution. For made shots, gamma power increased by 42.0% from pre-shot to execution.

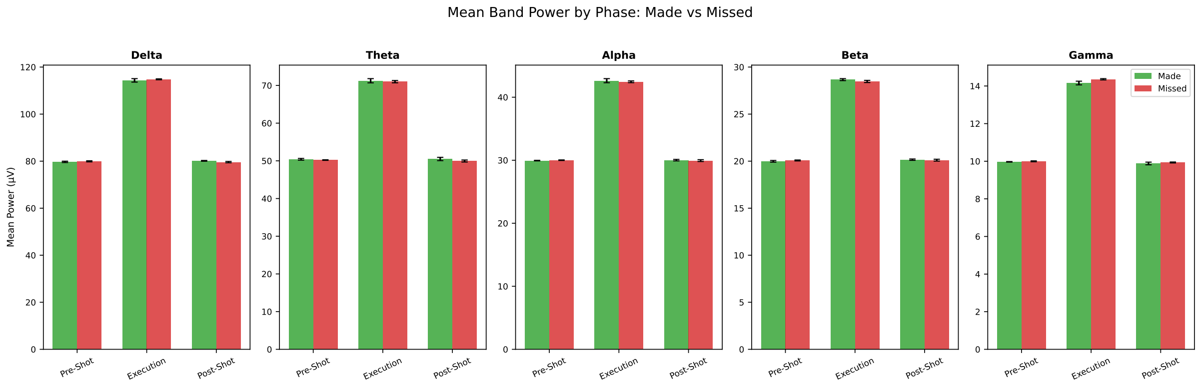

Figure 6: Mean band power by phase and outcome (± SEM).

3.7 Statistical Comparisons

Table 1 summarizes pre-shot band power for made and missed shots, along with inferential test results.

Table 1: Pre-shot band power: descriptive and inferential statistics.

Band	Made M (SD)	Missed M (SD)	t	p	U	d
Delta	79.7 (0.6)	79.9 (0.7)	-0.52	0.628	7	-0.34
Theta	50.4 (0.5)	50.2 (0.2)	0.67	0.560	12	0.64
Alpha	29.9 (0.1)	30.0 (0.1)	-0.86	0.427	5	-0.54
Beta	20.0 (0.2)	20.1 (0.1)	-0.74	0.510	8	-0.58
Gamma	10.0 (0.0)	10.0 (0.1)	-0.89	0.401	7	-0.45

3.8 Theta/Alpha Ratio

The pre-shot theta/alpha ratio has been proposed as an index of focused attention in sport performance.. Mean pre-shot θ/α ratio was 1.68 (SD $=$ 0.02) for made shots and 1.67 (SD $=$ 0.01) for missed shots. Made shots showed a higher θ/α ratio, differing by 0.01.

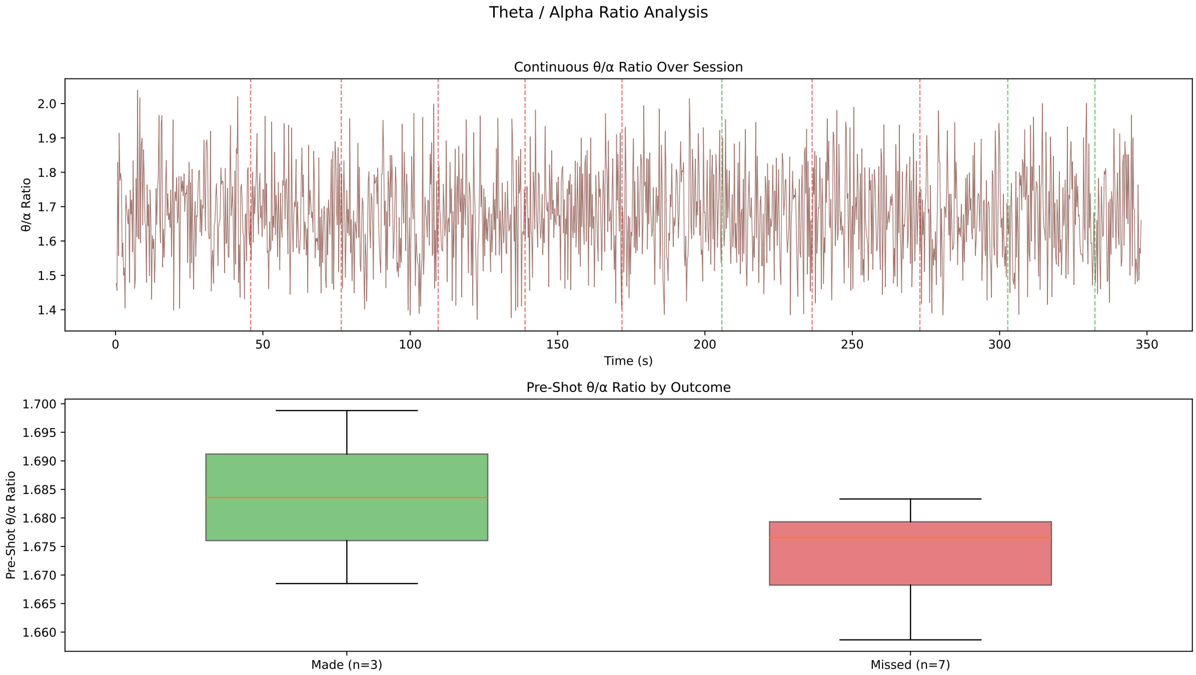

Figure 7: (Top) Continuous θ/α ratio over the session. (Bottom) Pre-shot θ/α ratio by outcome.

3.9 Shot-by-Shot Progression

Figure 8 tracks pre-shot band power across the 10 shots. Pre-shot alpha power showed a trend toward increase across the session ($r = 0.14$, $p = 0.708$), though the correlation was weak, possibly due to the limited number of trials.

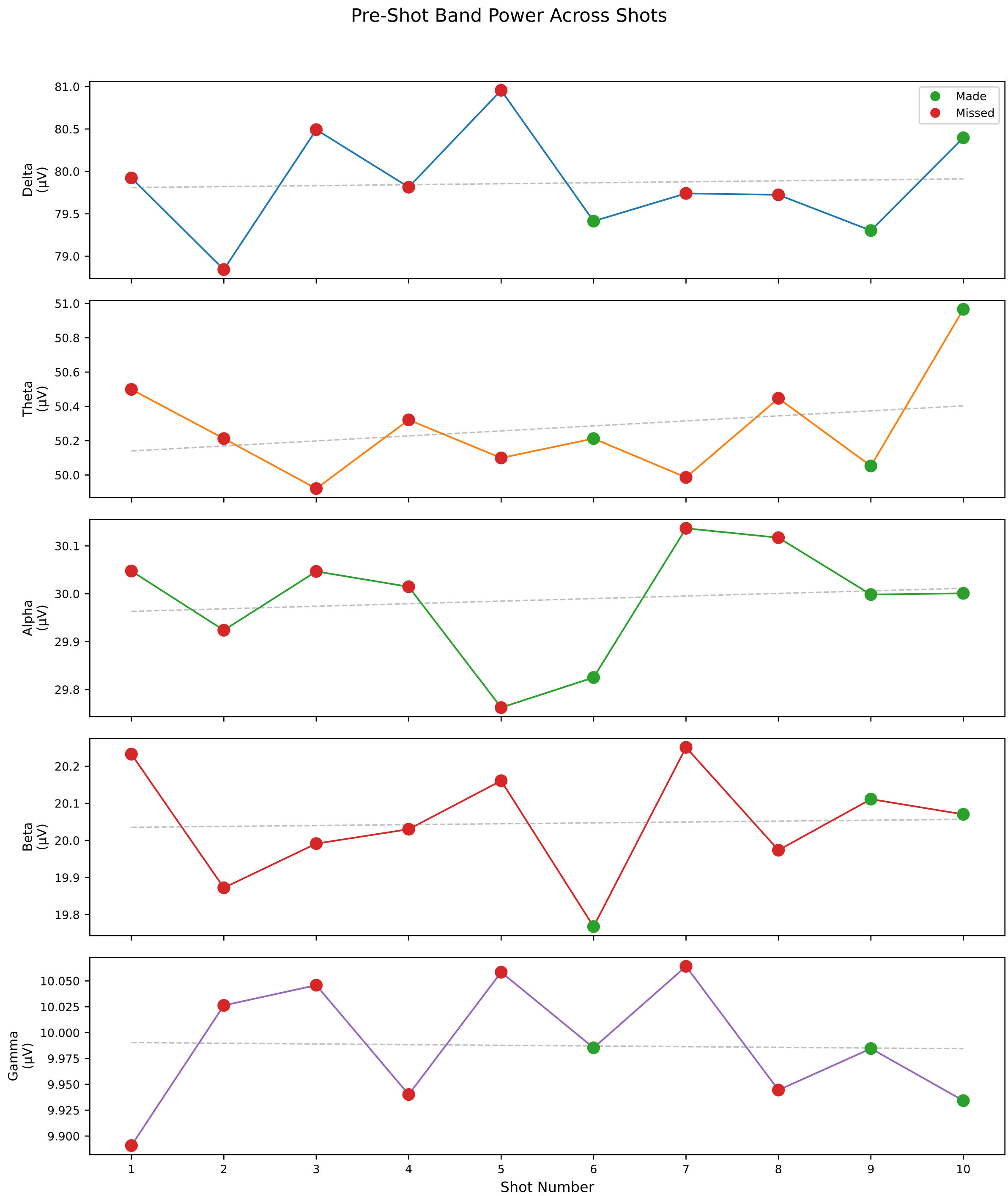

Figure 8: Pre-shot band power across shots. Dot colour indicates outcome (green = made, red = missed). Dashed line shows linear trend.

4 Video and Pose Estimation Analysis

In addition to EEG, the session video was recorded continuously at 30 fps (640×480 resolution). Post-hoc pose estimation was performed using MediaPipe Pose (heavy model) to extract 33 body landmarks per frame. Biomechanical features—elbow angle, wrist height, knee angle, and body lean angle—were computed across the shot execution phase for each trial and compared between made and missed shots.

4.1 Shot Stop-Motion Montage

Figure 9 presents a frame-by-frame stop-motion decomposition of each shot during the execution phase, with pose skeleton overlays. Made shots are shown in the upper rows (green borders) and missed shots in the lower rows (red borders).

Figure 9: Stop-motion montage of all shots during the execution phase. Pose skeleton overlays are drawn semi-transparently. Border colour indicates outcome (green = made, red = missed).

4.2 Ghost Shot Overlay

Figure 10 shows composite "ghost" images created by pixel-averaging the release-point frames across made and missed shots separately (top row), along with skeleton-only overlays showing individual shot pose variability (bottom row).

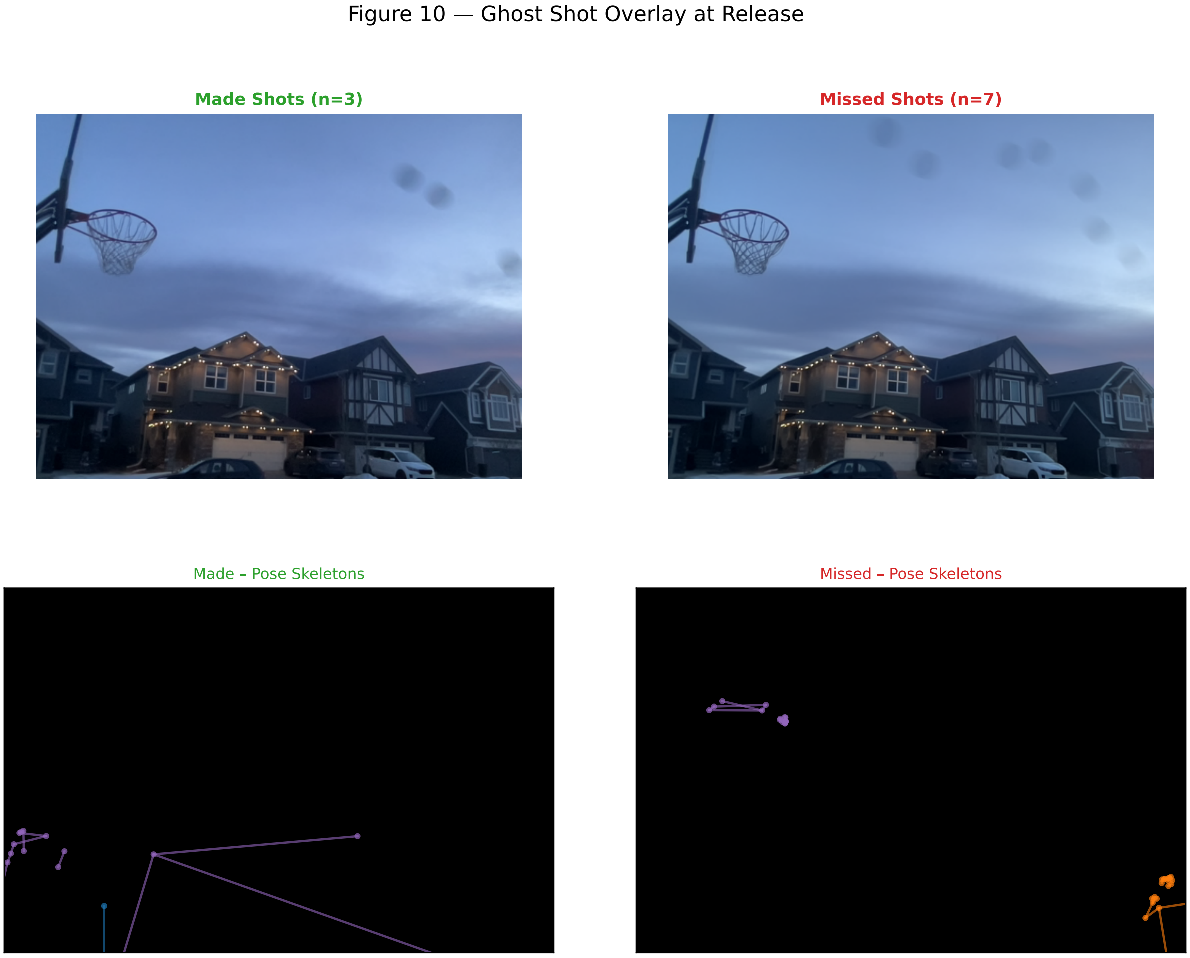

Figure 10: Ghost overlay composites at the estimated release point. Top: pixel-averaged frames for made (left) and missed (right) shots. Bottom: skeleton-only overlays with individual shots in distinct colours.

4.3 Pose Kinematics Trajectories

Figure 11 plots the time course of four biomechanical features during the execution phase, comparing made (green) and missed (red) shots. Peak elbow angle was lower for made shots (167.4) than missed (178.5). Peak wrist height was higher for made shots (0.5) than missed (0.2). Peak knee angle was lower for made shots (177.0) than missed (179.4). Peak body lean was higher for made shots (88.8) than missed (43.6).

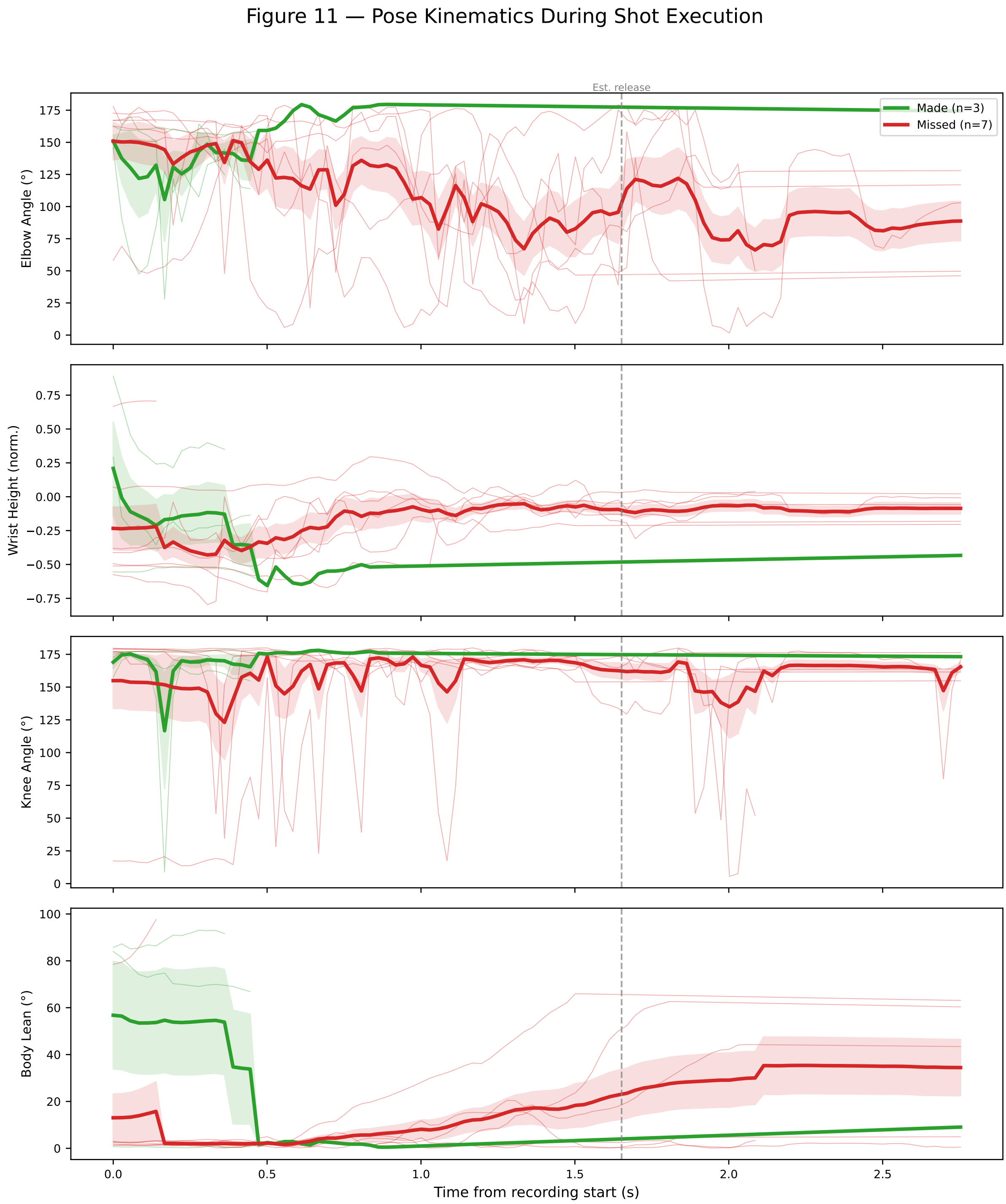

Figure 11: Biomechanical feature trajectories during shot execution (mean ± SEM). Thin lines show individual shots; thick lines show group means. Dashed vertical line: estimated release point.

4.4 Integrated Pose and EEG Analysis

Figure 12 presents a joint visualization of pose kinematics (elbow angle, wrist height) and EEG dynamics (alpha power, θ/α ratio) during the execution phase, time-aligned to recording onset. Time-aligned visualization of pose and EEG data during execution reveals concurrent motor and neural dynamics. Cross-domain correlations between mean pose features and alpha power are annotated where available.

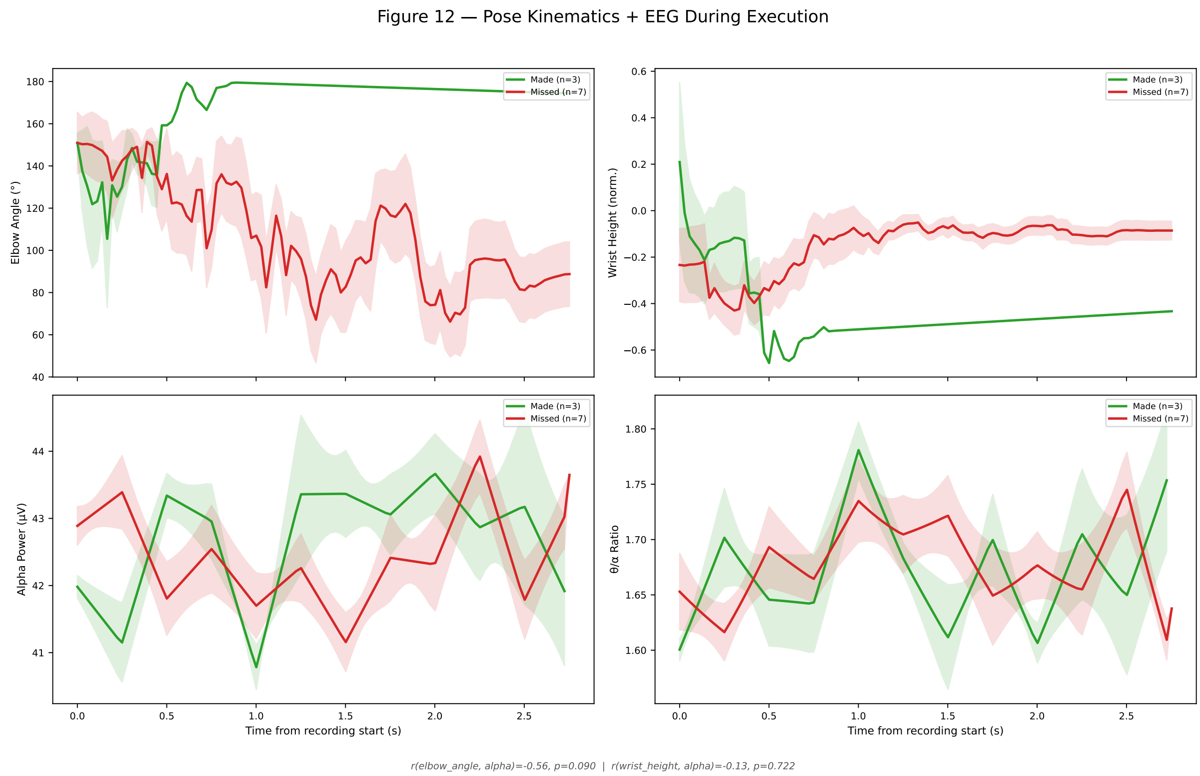

Figure 12: Combined pose kinematics and EEG dynamics during shot execution. Top row: elbow angle and wrist height. Bottom row: alpha band power and θ/α ratio. All traces show made (green) vs. missed (red) mean $\pm$ SEM.

4.5 Average Frame Composites

Figure 13 shows pixel-averaged video frames at three time points (start, midpoint, end) of the execution phase for made and missed shots, with an absolute difference image highlighting regions of greatest divergence.

Figure 13: Average frame composites. Top row: made shots. Middle row: missed shots. Bottom row: absolute pixel difference. Columns correspond to execution start, midpoint, and end.

5 Discussion

This pilot session (10 shots, 30% accuracy) provides an initial demonstration that the FreethrowEEG system can capture frequency-band-specific EEG dynamics during free-throw shooting.

Medium-to-large effect sizes were observed for pre-shot power in theta ($d = 0.64$), alpha ($d = -0.54$), beta ($d = -0.58$), suggesting these bands may carry performance-relevant information even in a small sample.

The shot-by-shot progression analysis provides a preliminary look at temporal dynamics across the session. Changes in band power over successive shots may reflect fatigue, adaptation, or strategy adjustment, though the current data cannot distinguish between these.

Video-based pose estimation using MediaPipe revealed descriptive differences in shooting kinematics between made and missed shots. Stop-motion decomposition and ghost-overlay composites provide visual evidence of form consistency, while time-aligned pose and EEG traces offer a preliminary window into the brain–body dynamics underlying free-throw execution.

5.1 Limitations

This analysis is based on a single pilot session with 10 shots (3 made), which severely limits statistical power. The Muse 2 provides only four channels, precluding source localization or detailed topographic analysis. Band power values represent averages across all channels, which may obscure hemisphere-specific effects. Future sessions with larger sample sizes are needed to draw reliable conclusions.

6 Conclusion

This pilot analysis demonstrates that the FreethrowEEG system can successfully record and analyse EEG band power during free-throw shooting with a portable Muse headset. Exploratory analyses identified Delta, Theta, Alpha, Beta, Gamma band power as potentially differentiating made from missed shots. The addition of video-based pose estimation provides a complementary kinematic dimension, enabling time-aligned analysis of brain and body dynamics during shot execution. Ghost overlays and average frame composites offer intuitive visual summaries of shooting form variability. These results provide a foundation for larger-scale data collection and more rigorous hypothesis testing.